Adaptation to the spindle checkpoint is regulated by the interplay between Cdc28/Clbs and PP2A^{Cdc55}

Claudio Vernieri, Elena Chiroli, Valentina Francia, Fridolin Gross, and Andrea Ciliberto

FIRC Institute of Molecular Oncology (IFOM), 20139 Milan, Italy

The spindle checkpoint arrests cells in metaphase until all chromosomes are properly attached to the chromosome segregation machinery. Thereafter, the anaphase promoting complex (APC/C) is activated and chromosome segregation can take place. Cells remain arrested in mitosis for hours in response to checkpoint activation, but not indefinitely. Eventually, they adapt to the checkpoint and proceed along the cell cycle. In yeast, adaptation requires the phosphorylation of APC/C. Here, we show that the protein phosphatase PP2A^{Cdc55} dephosphorylates APC/C, thereby counteracting the activity of the mitotic kinase Cdc28. We also observe that the key regulator of Cdc28, the mitotic cyclin Clb2, increases before cells adapt and is then abruptly degraded at adaptation. Adaptation is highly asynchronous and takes place over a range of several hours. Our data suggest the presence of a double negative loop between PP2A^{Cdc55} and APC/C^{Cdc20} (i.e., a positive feedback loop) that controls APC/C^{Cdc20} activity. The circuit could guarantee sustained APC/C^{Cdc20} activity after Clb2 starts to be degraded.

Introduction

During metaphase, chromosomes consist of pairs of sister chromatids held together by the cohesin complex. Cohesin cleavage by the protease separase is the essential step that starts the physical separation of sister chromatids and drives cells into anaphase (Nasmyth, 2002). For separase to cleave cohesin, cells need to degrade securin (Pds1 in *Saccharomyces cerevisiae*), the stoichiometric inhibitor of the protease. Degradation of Pds1 is mediated by the proteasome after ubiquitination by the essential E3 ubiquitin ligase anaphase promoting complex or cyclosome (APC/C) bound to its cofactor Cdc20 (Primorac and Musacchio, 2013). Degradation of Pds1 is insufficient, however, to guarantee exit from mitosis, which also requires the inactivation of the mitotic kinase cyclin-dependent kinase 1 (CDK1; Cdc28 in *S. cerevisiae*; Drapkin et al., 2009). Cdc28 inhibition occurs via the degradation of mitotic cyclins (Clbs, primarily Clb2 in budding yeast), an event that is initiated by APC/C^{Cdc20} and is completed by another complex APC/C^{Cdh1}, where Cdh1 is a second cofactor that replaces Cdc20 as cells enter anaphase (Primorac and Musacchio, 2013).

A surveillance pathway known as the spindle checkpoint prevents APC/C^{Cdc20} activation in the presence of as few as one kinetochore unattached to spindle microtubules (Rieder et al., 1995; Lara-Gonzalez et al., 2012). As a consequence of checkpoint activation, Cdc20 is sequestered in the mitotic checkpoint complex (MCC), which is composed of Cdc20 itself and three components of the checkpoint pathway: Mad2, Mad3 (BubR1 in mammals), and Bub3. Cdc20 in the MCC binds to APC/C, but APC/C^{MCC} is unable to recognize Pds1 and Clb2 (Lara-Gonzalez et al., 2012). After all kinetochores are properly attached to microtubules, the checkpoint is disengaged, MCC dissociates, APC/C^{Cdc20} is activated, and cells can transit into anaphase.

Remarkably, the lifting of checkpoint-inducing stimuli is not strictly required for cells to enter anaphase. When the checkpoint is constantly induced, cells can adapt to the checkpoint and progress into the cell cycle after several hours of metaphase arrest (Rudner et al., 2000; Brito and Rieder, 2006; Rossio et al., 2010). How APC/C is activated in the presence of stimuli that induce Cdc20 sequestration, and thus APC/C inhibition, is still not completely understood.

In vertebrates, the mechanism of adaptation has been ascribed to a slow, APC/C-dependent degradation of cyclin B (thus the phenomenon is also known as slippage) taking place in cells arrested by the spindle checkpoint (Brito and Rieder, 2006). When cyclin B drops below a critical level, CDK1 is

Correspondence to Andrea Ciliberto: andrea.ciliberto@ifom.eu

Abbreviations used in this paper: APC/C, anaphase promoting complex or cyclosome; IF, immunofluorescence; MCC, mitotic checkpoint complex.

The Rockefeller University Press $30.00
J. Cell Biol. Vol. 202 No. 5 765–778
www.jcb.org/cgi/doi/10.1083/jcb.201303033

inactivated, and cells can no longer sustain the mitotic state leading to exit from mitosis.

The molecular mechanisms by which Cdc28/CDK1 inhibition could induce APC/C^{Cdc20} activation, and transition into anaphase and adaptation, are not entirely clear. In mammals, CDK1 sustains the checkpoint (D'Angiolella et al., 2003; Morin et al., 2012) and thus indirectly inhibits APC/C^{Cdc20}. It has therefore been proposed that CDK1 inactivation relieves the inhibition of APC/C^{Cdc20} exerted by the checkpoint and facilitates the transition to anaphase (Zeng et al., 2010; He et al., 2011).

A role for Cdc28 in maintenance of the spindle checkpoint, and thus in the inhibition of APC/C^{Cdc20}, has also been proposed in budding yeast (Li and Cai, 1997; Kitazono et al., 2003). However, in this organism Cdc28 has also a role in promoting APC/C^{Cdc20} activity. Cdc28 activates APC/C by phosphorylating two of its subunits (Cdc16 and Cdc27), and thus favoring APC/C binding with Cdc20 (Rudner and Murray, 2000). Moreover, Cdc28 activity is required for the expression of Cdc20 during metaphase arrest (Liang et al., 2012). In summary, in yeast Cdc28 is reported to contribute to both APC/C^{Cdc20} inhibition, indirectly via the checkpoint, and to APC/C^{Cdc20} activation via APC phosphorylation and production of Cdc20 (Fig. 1 A). It is thus unclear whether Cdc28 activity promotes or inhibits metaphase arrest in cells subjected to a prolonged checkpoint stimulus.

Similarly, the relationship between APC/C^{Cdc20} activation and phosphatases during adaptation to the spindle checkpoint is not fully understood. Based on the premise that Cdc28 is involved in spindle checkpoint maintenance, Cdc14, its main opposing protein phosphatase (Rock and Amon, 2009), should favor checkpoint silencing and APC/C^{Cdc20} formation. Indeed, the overexpression of Cdc14 silences the checkpoint in a Cdc20-dependent manner, and Cdc14 prevents checkpoint reactivation in anaphase (Mirchenko and Uhlmann, 2010). It is unknown, however, whether physiological levels of Cdc14 have a role in promoting adaptation. This is not obvious, as Cdc14 is primarily required for events that follow anaphase and it is only fully activated well after APC/C^{Cdc20} has been activated.

Phosphatase $PP2A^{Cdc55}$ (i.e., the type 2A phosphatase bound to its regulatory domain Cdc55) instead inhibits metaphase-to-anaphase transition: $PP2A^{Cdc55}$ activity drops when cells enter anaphase (Queralt et al., 2006), whereas *cdc55Δ* mutants are checkpoint deficient (Minshull et al., 1996). During an unperturbed cell cycle, $PP2A^{Cdc55}$ delays anaphase onset by inhibiting the release of Cdc14 from the nucleolus where it is bound to Net1 (Queralt et al., 2006; Wang and Ng, 2006; Yellman and Burke, 2006) and by inhibiting separase (Clift et al., 2009). Whether $PP2A^{Cdc55}$ has a similar role in inhibiting adaptation is unknown.

In this manuscript, we explore possible mechanisms of APC/C activation in cells arrested by the spindle checkpoint in budding yeast. We show that transition to anaphase in adaptation: (1) requires APC/C phosphorylation and Cdc28/Clbs activity; (2) is opposed by $PP2A^{Cdc55}$ via APC/C dephosphorylation; (3) is variable in length; and (4) does not require Cdc14. Finally, we suggest the presence of a positive feedback loop that allows a rapid transition from metaphase arrest to anaphase during adaptation to the spindle checkpoint.

Results

Cdc20 and APC/C phosphorylation, but not Cdh1, are required for adaptation to the spindle checkpoint

APC/C is activated both by posttranslational modifications and by association with the cofactors Cdc20 and Cdh1. We asked which of these mechanisms is required for budding yeast cells to adapt to a prolonged checkpoint stimulus. To this aim, we compared the kinetics of the metaphase-to-anaphase transition in adapting cells (1) expressing nonphosphorylatable mutants for two subunits of the APC/C, Cdc27 (*cdc27-5A*) and Cdc16 (*cdc16-6A*); (2) deleted for *CDH1*; and (3) depleted of Cdc20.

In principle, we could have induced the spindle checkpoint by treating cells with tubulin-depolymerizing drugs like nocodazole. However, we observed that the effects of nocodazole begin to wear off after 5–6 h, and thus transition to anaphase after tubulin repolymerization and microtubule/kinetochore attachment can easily be mistaken for adaptation. We thus induced checkpoint activation by overexpressing one of its essential components, Mad2. We used yeast cells containing three copies of the *MAD2* gene under the control of the inducible *GAL1* promoter (*GAL1-MAD2 (3X)*; Rossio et al., 2010). Addition of galactose to the medium of these cells switches on the *GAL1* promoter and causes Mad2 to accumulate to a level that ectopically induces MCC formation, similarly to nocodazole (Mariani et al., 2012).

GAL1-MAD2 (3X) cells adapted to the checkpoint after several hours of growth in galactose. Adaptation was marked by the degradation of Clb2 and Pds1, and by the elongation of mitotic spindles, in agreement with previously published data (Rossio et al., 2010; Fig. 1, B and C). The presence of nonphosphorylatable subunits of APC/C prevented adaptation, with *GAL1-MAD2 (3X) cdc16-7A cdc27-5A* cells displaying persistently high levels of Clb2 and Pds1 (Fig. 1 D), and a large majority of metaphase spindles after several hours (Fig. 1 C). When grown in glucose, *GAL1-MAD2 (3X) cdc16-7A cdc27-5A* completed one cell cycle with kinetics that were only slightly delayed compared with *GAL1-MAD2 (3X)* cells (Fig. S1 A). These results are in agreement with data from Rudner and Murray (2000), who analyzed the growth of APC mutants in solid media under checkpoint-inducing conditions.

We next assessed the requirement of the cofactors Cdc20 and Cdh1 in adaptation to the spindle checkpoint. Given the essential role of Cdc20 in the metaphase-to-anaphase transition, it was not surprising that depletion of Cdc20 impaired adaptation to the checkpoint (Fig. S1 B). The role of *CDH1*, a nonessential gene in the metaphase-to-anaphase transition, was harder to predict. Because it was difficult to synchronize *GAL1-MAD2 (3X) cdh1Δ* cells in G1, we tested their ability to adapt to the spindle checkpoint using a cycling population. Our results show that *GAL1-MAD2 (3X) cdh1Δ* cells assembled and disassembled metaphase spindles very similarly to *GAL-MAD2 (3X)* cells, thus excluding a fundamental role for Cdh1 in adaptation (Fig. 1 E).

We conclude that although Cdh1 is dispensable for adaptation to the spindle checkpoint, both Cdc20 and phosphorylation of the APC/C subunits Cdc16 and Cdc27 are essential.

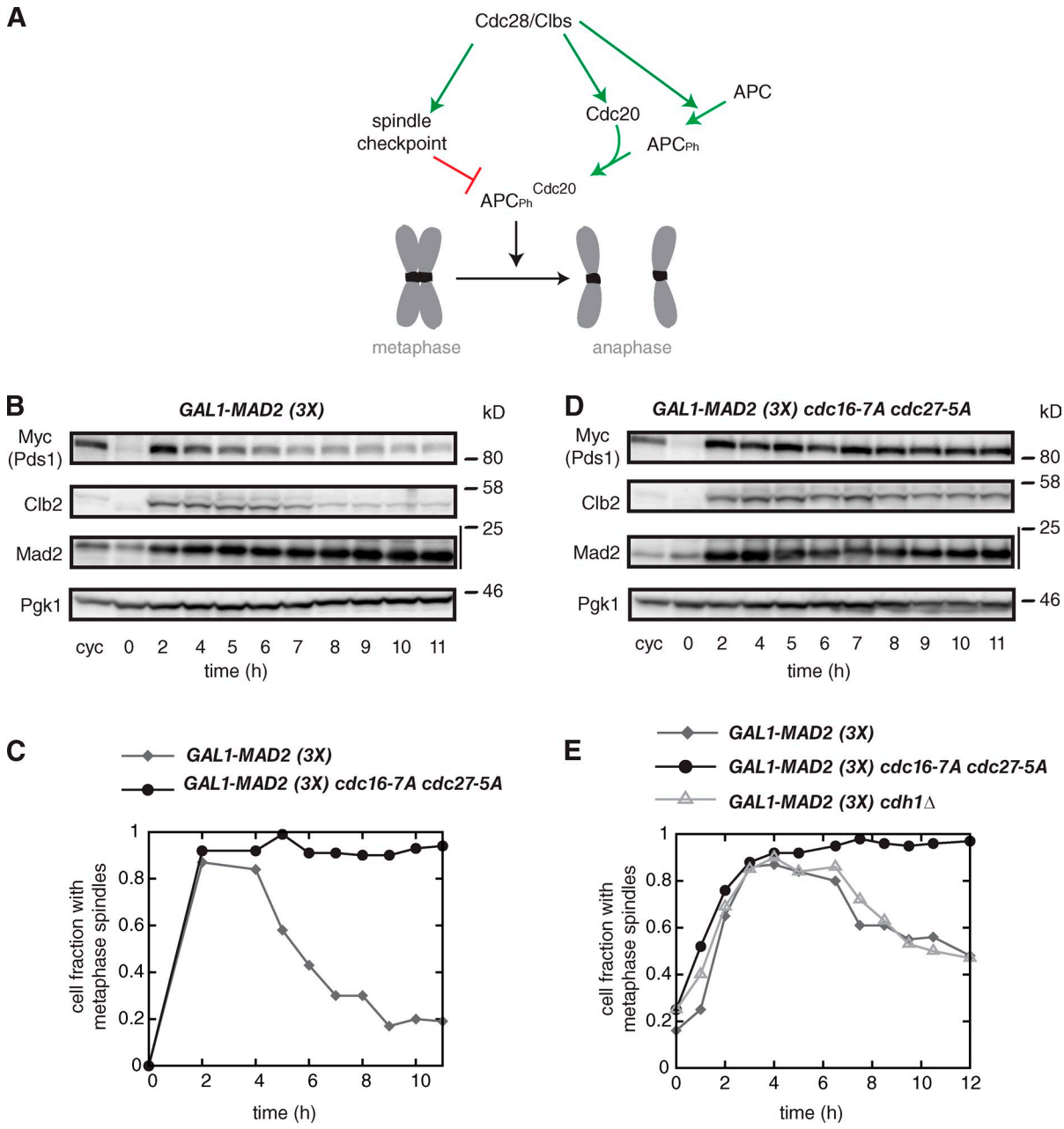

Figure 1. **Cdh1 is dispensable for the adaptation to the spindle checkpoint.** (A) Cdc28/Clbs trigger a chain of events that both promote (green) and inhibit (red) transition to anaphase. (B–D) *GAL1-MAD2 (3X)* (yAC489) and *GAL1-MAD2 (3X) cdc27-5A cdc16-6A* (yAC1675) cells were synchronized in G1 with α-factor and released in galactose-containing medium. 2 h after the release, α-factor was re-added. Samples were taken for Western blotting (B and D) and IF analysis (IF; C) with anti-tubulin antibodies. The data shown in C are from a single representative experiment out of three repeats. For the experiment shown, $n = 100$. (E) *GAL1-MAD2 (3X)* (yAC489), *GAL1-MAD2 (3X) cdh1Δ* (yAC1738), and *GAL1-MAD2 (3X) cdc27-5A cdc16-6A* (yAC1675) cells were grown at 30°C in YEPR and shifted to galactose. Samples were taken every hour and the proportion of metaphase spindles was measured by IF. The data shown are from a single representative experiment out of three repeats ($n = 100$).

Partial inhibition of Cdc28 does not overcome cell cycle arrest induced by the spindle checkpoint

The observation that Cdc20 is required for cells to adapt is at odds with the fact that Cdc20 is sequestered in the MCC when the checkpoint is operational. We thus asked what mechanism underlies the release of Cdc20 in adapting cells. Our data showed that Clb2 is slowly, but steadily, degraded during adaptation (Fig. 1 B). Cdc28 requires Clbs for its activity in mitosis, and Cdc28 has been proposed to be required for checkpoint activity. It is thus plausible that the slow degradation of Clb2 by decreasing Cdc28 activity leads to checkpoint inactivation, Cdc20 release from the MCC, and ultimately to adaptation via the formation of APC/C^{Cdc20}.

To verify this hypothesis, we asked whether it is possible to overcome the spindle checkpoint arrest in yeast by inhibiting Cdc28. To modulate Cdc28 activity, we used a mutant of *CDC28*, *cdc28-as1*, that can be inhibited by the ATP analogue 1-NMPP1 (Bishop et al., 2000). APC/C^{Cdc20} activity was monitored by the degradation of Pds1 and Clb2. Depending on the

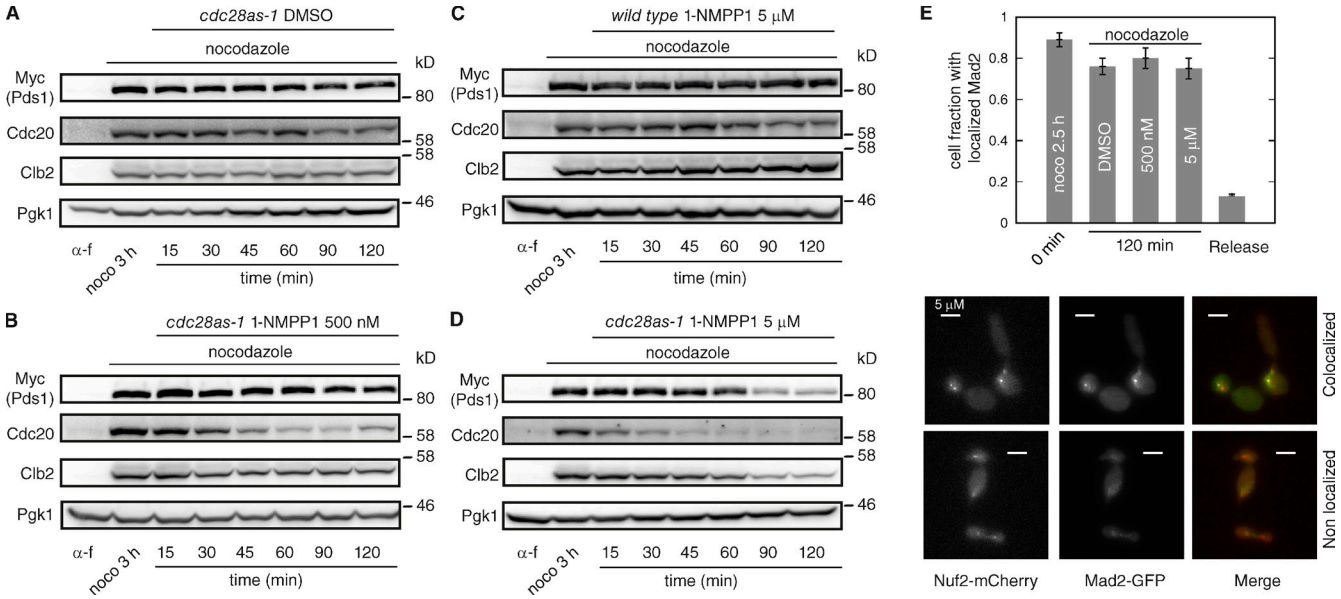

Figure 2. **Cdc28 inhibition causes a decrease of Cdc20 levels during a checkpoint arrest.** (A–D) *CDC28 PDS1-MYC18* (yAC359) and *cdc28-as1 PDS1-MYC18* (yAC779) cells were synchronized in G1 phase with α-factor and then released in YEPD supplemented with nocodazole. After 3 h in nocodazole, the indicated concentrations of 1-NMPP1 or DMSO were added together with 20 µg/ml of α-factor. Samples were taken at the indicated times after the addition of 1-NMPP1 or DMSO for Western blotting. (E, top) *cdc28-as1 MAD2-3GFP NUF2-mCherry* (yAC2182) cells were treated similarly to A–D: after 2.5 h in nocodazole (noco), cells were kept two additional hours in the presence of nocodazole supplemented with DMSO, 500 nM, or 5 µM 1-NMPP1 (120 min). One fraction of cells was instead released from nocodazole (Release). Colocalization of Mad2 with Nuf2 was scored at 120 min (see also Materials and methods); error bars refer to standard errors from three independent experiments. In each experiment, 50 cells were analyzed for each condition. (E, bottom) Examples of localized and nonlocalized Mad2.

amount of 1-NMPP1, Cdc28-as1 can be fully or partially inactivated (Bishop et al., 2000; Liang et al., 2012). We reasoned that partial inactivation would better mimic the initial stages of Cdc28 inactivation after Clb2 degradation in adaptation. For this reason, we used 500 nM 1-NMPP1, a concentration that allows DNA replication but arrests cells in a premitotic state (Bishop et al., 2000; Liang et al., 2012). We confirmed this by adding 500 nM 1-NMPP1 to *cdc28-as1* cells released from G1 arrest and measuring their DNA content by FACS and mitotic spindle assembly (Fig. S1, C and D).

cdc28-as1 cells were arrested in prometaphase by nocodazole for 3 h, and then treated with 500 nM 1-NMPP1. Having confirmed that nocodazole depolymerized spindles throughout the experiment (Fig. S1 E) and that cells arrested with a 2C DNA content (Fig. S1 F), we monitored cells for a further 2 h. We observed that APC/C was not reactivated toward Pds1 and Clb2, which were not destabilized, but Cdc20 levels rapidly decreased when compared with DMSO control (Fig. 2, A and B). The reduction in Cdc20 could be caused by its decreased synthesis or increased degradation. We favor the former hypothesis because Cdc28 inhibition arrests *CDC20* transcription (Liang et al., 2012), whereas Cdc20 is quickly degraded during checkpoint arrest, its degradation being dependent on APC/C (Pan and Chen, 2004).

Our results suggest that the checkpoint is still active, and thus APC/C^{Cdc20} is unable to target Pds1 and Clb2 after the partial inhibition of Cdc28. To confirm that this is the case, we repeated the experiment with a yeast strain carrying Mad2-GFP, which is recruited at kinetochores during a checkpoint-induced arrest (Gillett et al., 2004). Our results confirmed that the checkpoint pathway was still active at the kinetochores after Cdc28 inhibition, as Mad2-GFP colocalized with a component of the outer kinetochore, Nuf2, 2 h after treatment with 500 nM 1-NMPP1 (Fig. 2 E), like in the DMSO control. Cells released from nocodazole, which repolymerized mitotic spindles (Fig. S1 G), did not show kinetochore localization of Mad2 as expected.

The reduction of Cdc20 did not allow us to come to a conclusion about the status of the checkpoint pathway downstream of Mad2 after Cdc28 inhibition. To confirm that the pathway was still active, we repeated the experiment in cells where *CDC20* expression is not under the control of Cdc28. To this aim, we used cells deleted for *YOX1*, which produces an inhibitor of *CDC20* expression whose activity is down-regulated by Cdc28 (Liang et al., 2012). We observed that Cdc20 was stable in these cells for up to 1.5 h after the addition of 500 nM 1-NMPP1, whereas Pds1 and Clb2 levels remained unchanged, indicating that the checkpoint was still active after Cdc28 inhibition (Fig. S2 A and Fig. S2, B and C, for the functionality of the drug).

In summary, our results show that the inhibition of Cdc28 with 500 nM 1-NMPP1 is sufficient to keep the upstream spindle checkpoint pathway active, but unable to support the production of Cdc20. As a consequence, APC/C^{Cdc20} could not be activated and cells remained arrested in metaphase.

Strong inhibition of Cdc28 leads to Clb2 and Pds1 degradation independently from Cdc20

Previous results showed that Cdc28 inhibition during a spindle checkpoint–induced metaphase arrest leads to the degradation of Pds1 and Clb2, and separation of sister chromatids

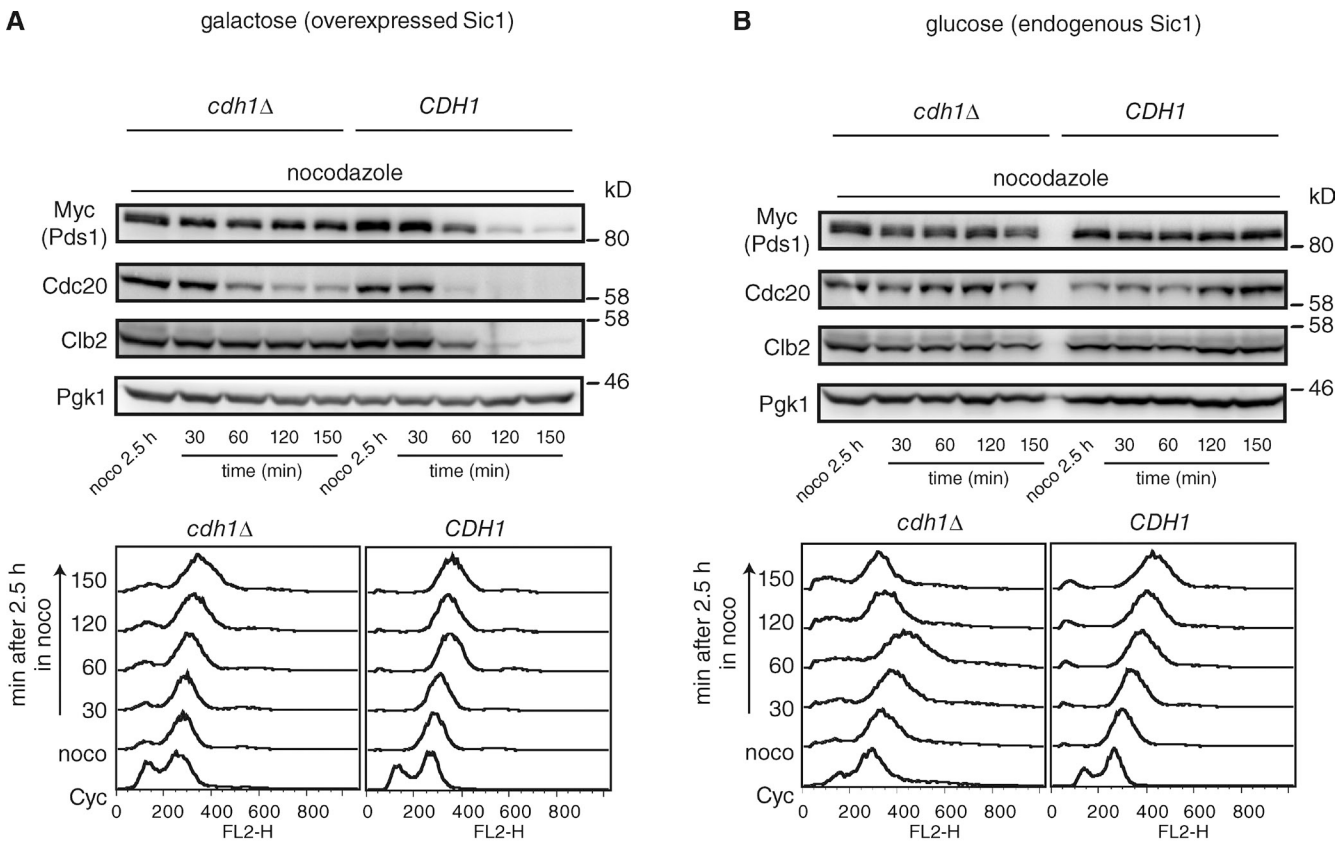

Figure 3. **Cdh1 is responsible for Pds1 and Clb2 degradation upon strong Cdc28 inhibition.** (A and B) *GAL-SIC1* (yAC2025) and *GAL-SIC1 cdh1Δ* (yAC2023) cells were grown in either raffinose (A) or glucose (B) at 23°C. When in log phase, nocodazole was added to the media for 2.5 h and then cells were either supplemented with galactose (A) or kept in glucose (B). Samples were analyzed by Western blotting (top) and FACS (bottom). The data are from a single representative experiment out of three repeats.

(Amon, 1997). We reasoned that the discrepancy between these published data and our results is most likely caused by the level of Cdc28 inhibition. Therefore, we increased the dose of 1-NMPP1 from 500 nM to 5 µM, a concentration that is known to also inhibit DNA replication (Bishop et al., 2000). To test the efficacy of the drug, we synchronized cells in G1 and released them in media supplemented with 5 µM 1-NMPP1. We confirmed that under these conditions, cells arrested with 1C DNA content for 2.5 h without forming metaphase spindles (Fig. S1, C and D). We then added 5 µM 1-NMPP1 to *MAD2-GFP NUF2-mCherry cdc28as-1* cells arrested in prometaphase by nocodazole. Similar to the results obtained with 500 nM 1-NMPP1, we observed that Mad2-GFP was largely localized at the kinetochores up to 2 h after the addition of 5 µM 1-NMPP1 (Fig. 2 E), which suggests that the checkpoint was not dismantled. However, at variance with results obtained with 500 nM 1-NMPP1, Pds1 and Clb2 levels decreased markedly after 1.5 h of treatment (Fig. 2 D). Cdc20 levels decreased even more rapidly after treatment with 5 µM 1-NMPP1, which implies that the reduction in Pds1 and Clb2 was not caused by APC/C^{Cdc20} (Fig. 2, C and D).

We conclude that although APC/C can be activated by strong inhibition of Cdc28, its activation does not require Cdc20 nor the inactivation of the upstream checkpoint pathway at the kinetochores.

Cdh1 is required for Clb2 and Pds1 degradation upon strong Cdc28 inhibition

We asked whether the degradation of Pds1 and Clb2 after strong inhibition of Cdc28 was caused by APC/C^{Cdh1}. This possibility is supported by evidence that Cdc28 inhibits Cdh1 (Zachariae et al., 1998). Unfortunately, we could not use *cdh1Δ* cells that carry the *cdc28as-1* allele because the two mutations are synthetic lethal. We thus inhibited Cdc28 activity by overexpressing the stoichiometric inhibitor Sic1 (Schwob et al., 1994), expressed under the *GAL1* promoter (Amon, 1997). We first confirmed that Sic1 overexpression efficiently inhibited Cdc28 activity in vivo (Fig. S2 D). We then arrested cells in prometaphase with nocodazole for 2.5 h, and afterward we induced Sic1 overexpression with galactose. Crucially, Clb2 and Pds1 were stable in *cdh1Δ* cells but were quickly degraded in cells carrying *CDH1* wild type (Fig. 3 A). Notice that cells are under nocodazole and thus unable to form microtubules: that is why they cannot undergo cytokinesis and exit mitosis regardless of the degradation of Pds1 and Clb2 (Fig. 3 A). This result confirms the hypothesis that APC/C^{Cdh1} is activated when Cdc28 is strongly inhibited. As expected, with physiological levels of Sic1, cells maintained the mitotic arrest with stable Pds1 and Clb2 independently of the presence of Cdh1 (Fig. 3 B). The degradation of Cdc20 in *cdh1Δ* cells is likely caused by the inhibition of its transcription after Cdc28 inactivation.

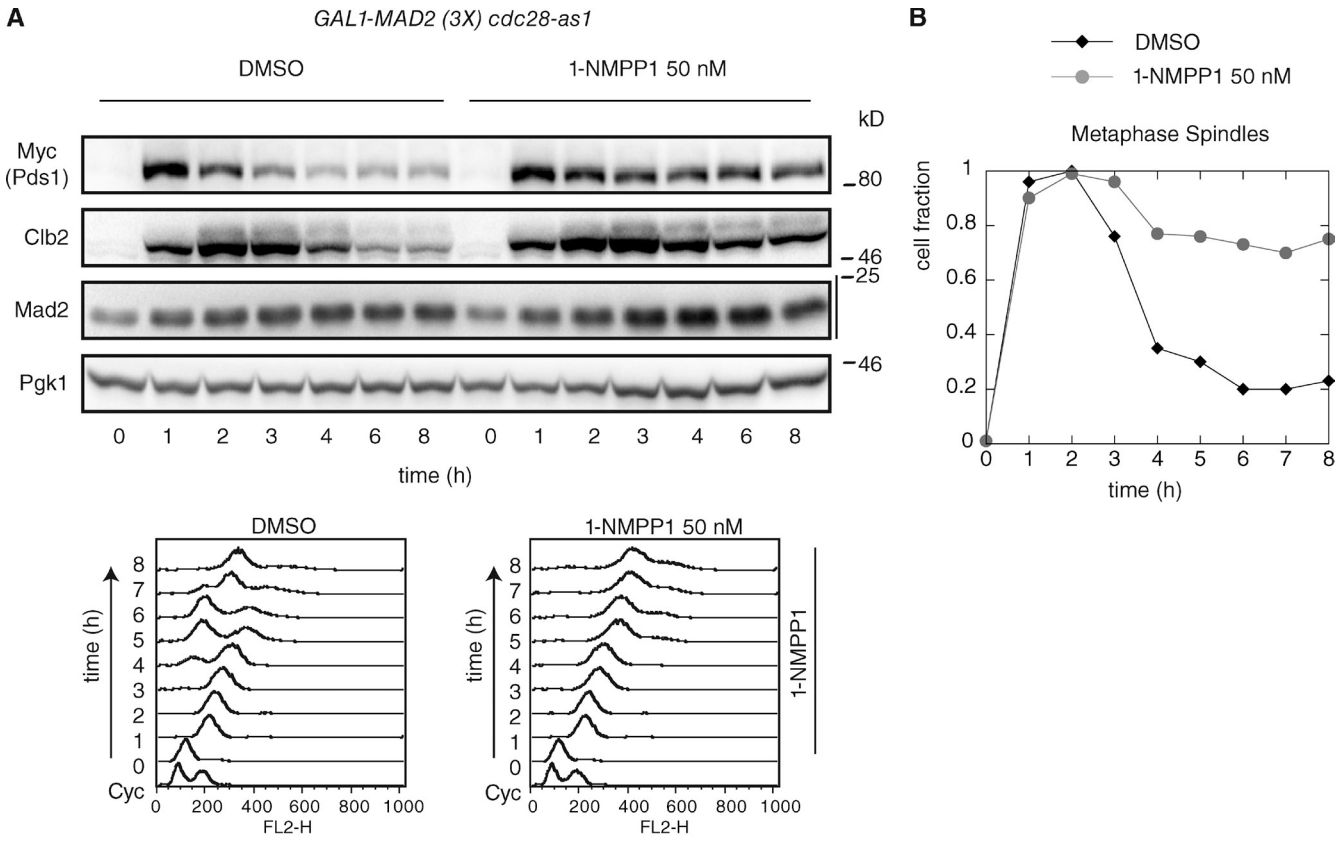

Figure 4. **A minimal amount of 1-NMPP1 significantly delays adaptation to the spindle checkpoint.** (A and B) *GAL1-MAD2 (3X) cdc28as-1 PDS1-MYC18* (yAC1788) cells were grown in YEPR, synchronized in G1 with α-factor, and released in galactose. 1.5 h after the release, α-factor was re-added together with either DMSO or 50 nM of 1-NMPP1. Samples were treated for Western blotting and FACS (A), and IF analysis (B). The data shown are from representative experiments out of three repeats (in B, $n = 100$).

We thus conclude that when Cdc28 activity is greatly reduced, APC/C^{Cdh1} is activated and degrades both Pds1 and Clb2. Although Pds1 and Clb2 were degraded, it would be wrong to conclude from these data that adaptation requires APC/C^{Cdh1} activation mediated by a strong inactivation of Cdc28, as we have previously shown Cdh1 to be dispensable for adaptation (Fig. 1 E).

Cdc28 activity is required for cells to adapt

The experiments performed on cells arrested in prometaphase by nocodazole suggest that cells do not adapt to the checkpoint by inhibiting Cdc28 activity. We thus decided to test the opposite scenario, where Cdc28 activity is required for adaptation. In this scenario, it would be possible to inhibit adaptation by inhibiting Cdc28 with a minimal amount of ATP analogue sensitivity. To test this prediction, we assessed the effect of as little as 50 nM 1-NMPP1 on adaptation to a checkpoint arrest induced by Mad2 overexpression. *GAL1-MAD2 (3X) cdc28-as1* cells were synchronized in G1 by α-factor and released in galactose to induce Mad2 overexpression. Under control conditions (DMSO), the majority of cells adapted within 5 h (Fig. 4 A, left; and Fig. 4 B); however, in the presence of 50 nM 1-NMPP1, adaptation was inhibited in the vast majority of cells (Fig. 4 A, right; and Fig. 4 B). At this low concentration of 1-NMPP1, no effects were observed on cells expressing wild-type *CDC28* (Fig. S3, A and B). Moreover, when *GAL1-MAD2 (3X) cdc28-as1* cells were grown in a medium lacking galactose and therefore were not checkpoint arrested, 50 nM 1-NMPP1 induced only a small delay in the transition to anaphase as detected by spindle dynamics and FACS (Fig. S3 C).

We conclude therefore that in budding yeast Cdc28 activity is required for adaptation to the spindle checkpoint.

Clb2 levels increase constantly during a checkpoint-induced arrest and are rapidly reduced during the transition to anaphase

The notion that active Cdc28 is required for adaptation prompted us to reconsider the observation that Clb2, which is required for Cdc28 activity, is slowly degraded as cells adapt (Fig. 1 B). We reasoned that Western blots might mask the real nature of adaptation taking place in individual cells. We thus resorted to single cell analysis and followed the dynamics of Clb2 in yeast strains in which the mitotic cyclin was tagged with GFP (Hood et al., 2001).

Asynchronous *GAL1-MAD2 CLB2-GFP TUB2-Cherry* cells were loaded in flow chambers in the presence of galactose, and after a short time they arrested as budded cells in metaphase. We then followed adaptation in individual cells (Fig. 5 A), and the results were doubly surprising. Not only did we observe that Clb2 increased constantly during metaphase arrest, but the mitotic cyclin was also degraded very rapidly when cells

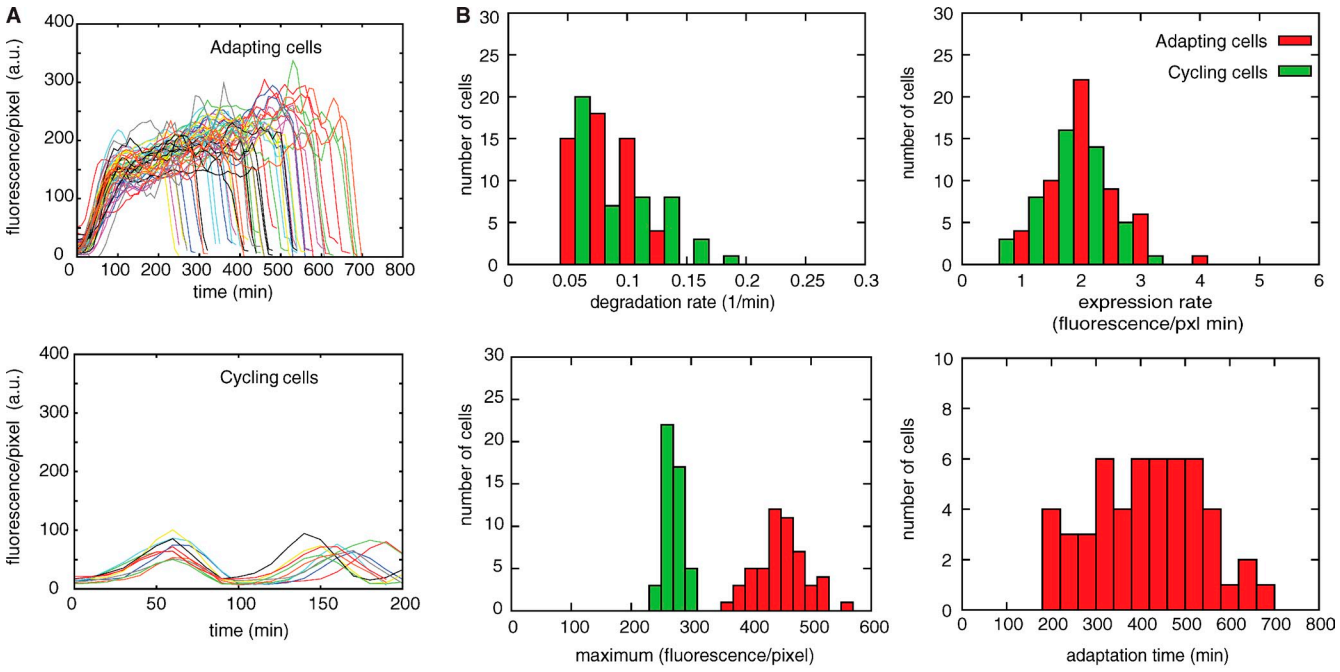

Figure 5. **Single cell analysis of adapting cells.** (A) *CLB2-GFP TUB2-Cherry GAL1-MAD2 (3X)* (yAC1732) cells were grown at 30°C in synthetic medium containing raffinose, and then were either shifted to galactose (adapting cells; top) or left in raffinose (cycling cells; bottom). We show Clb2-GFP accumulation signal in the nucleus after smoothing (see Materials and methods). Individual traces are synchronized at the time when Clb2 starts increasing. (B) Top left, degradation rate of Clb2; top right, expression rate, i.e., the rate of Clb2 accumulation; bottom right, adaptation time; bottom left, maxima of Clb2 fluorescence. See also Fig. S4, Materials and methods, and Video 1. The data shown are from a single representative experiment out of three repeats. For the experiment shown, $n = 50$. Cells were analyzed with the aid of the program phyloCell, written by G. Charvin (unpublished data).

adapted and entered anaphase. More precisely, Clb2 nuclear accumulation was constant and biphasic. Initially, Clb2 increased with a similar rate as in dividing cells (Fig. S4 A, bottom; and Fig. 5 B, top right), then the rate of increase slowed down, although Clb2 kept on increasing. On average, adapting cells accumulated about twice as much nuclear Clb2 as cycling cells (Fig. 5 A and Fig. 5 B, bottom left). The phase of slow Clb2 increase lasted until cells adapted. Entry into anaphase, detected by the elongation of mitotic spindles, occurred together with the rapid degradation of Clb2, which resulted in complete loss of the total protein in 20–30 min. The rate of Clb2 degradation was comparable to the rate of degradation in dividing cells (Fig. 5 B, top left; and Fig. S4 A, top). Crucially, adaptation times (i.e., the time between the beginning of Clb2 accumulation and spindle elongation) were extremely variable within the cell population, spanning over a period of 500 min (Fig. 5 B, bottom right).

It is likely that the slow degradation of Clb2 observed in Western blots is caused by asynchrony in adaptation times, which masked the rapid nature of Clb2 degradation in individual cells. When we repeated the experiments inducing the spindle checkpoint with nocodazole, we observed a similar behavior (Fig. S4 C, top) in cells that underwent adaptation before nocodazole ceased to inhibit the polymerization of tubulin (Fig. S4 C, bottom). Thus, Clb2 dynamics observed during Mad2 overexpression are a bona fide representation of what happens when the spindle checkpoint is induced by impairing microtubule–kinetochore attachment.

In conclusion, Clb2 concentration increases, and does not decrease, before cells adapt in budding yeast. Moreover, the sudden and stochastic activation of APC/C, and not its residual activity, drives the transition to anaphase during adaptation.

The PP2A^{Cdc55} phosphatase opposes Cdc16 phosphorylation during checkpoint arrest

We next asked why Cdc28 activity is necessary for adaptation (Fig. 4 A). We have already shown that phosphorylation of the APC/C subunits, Cdc16 and Cdc27, is required for adaptation (Fig. 1 D); therefore, it is possible that Cdc28 is needed to phosphorylate APC/C during adaptation. This notion is supported by published data showing that the two APC/C subunits are phosphorylated by Cdc28 when cells enter anaphase (Rudner and Murray, 2000). We confirmed that before adaptation Cdc16 is progressively phosphorylated, as detected by Western blotting using Phos-tag reagent (Fig. S5, A and B).

We reasoned that a phosphatase might oppose the increasing Cdc28/Clb2 activity during adaptation because cells took several hours to adapt despite accumulation of Clb2 in the nucleus. If Cdc28-mediated phosphorylation of APC/C is a key molecular event in overcoming the checkpoint arrest, then the phosphatase that dephosphorylates APC/C should be required to maintain arrest. A plausible candidate that could be responsible for APC/C dephosphorylation is the phosphatase PP2A^{Cdc55}, as *cdc55Δ* cells are checkpoint deficient (Minshull et al., 1996). Indeed, we confirmed that *GAL1-MAD2 (3X) cdc55Δ* cells do not undergo spindle checkpoint–induced arrest triggered by Mad2 overexpression (Fig. S5 C). We thus decided to test whether PP2A^{Cdc55} controls the phosphorylation state of APC/C during nocodazole-induced arrest.

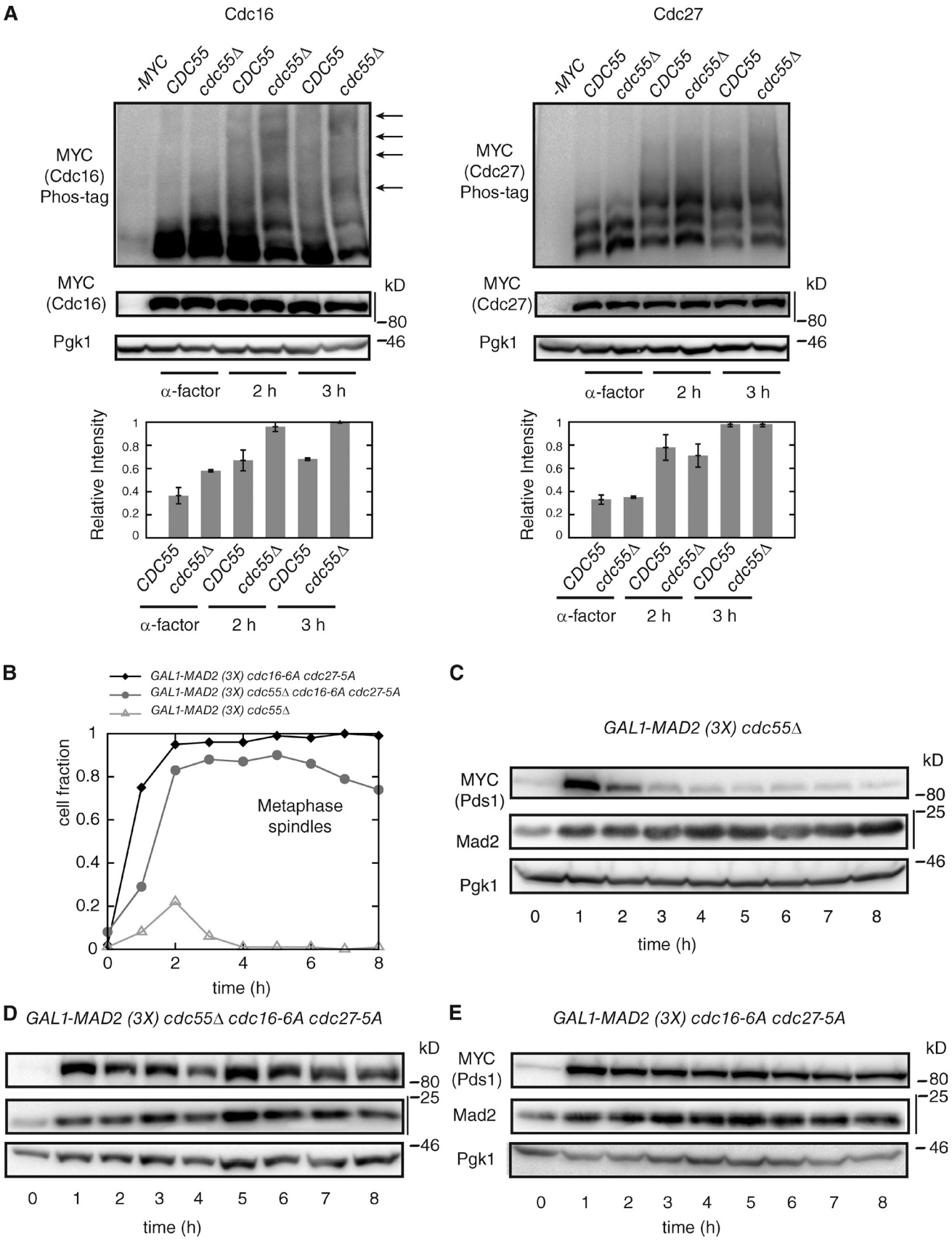

Figure 6. **PP2A^{Cdc55}-mediated dephosphorylation of APC subunits is essential for spindle checkpoint activity.** (A) *CDC16-myc6* (yAC1936), *CDC16-myc6 cdc55Δ* (yAC1994), *CDC27-myc9* (yAC1863), and *CDC27-myc9 cdc55Δ* (yAC1888) cells were grown in YEPD at 30°C, arrested in G1 phase, and released in nocodazole. Samples were taken during the G1 arrest and after 2 and 3 h for Western blotting analysis of Cdc16 (left) and Cdc27 (right) using Phos-tag

We compared the Western blot profiles of Cdc16 and Cdc27 in *CDC55* wild-type and *cdc55Δ* cells after releasing them from a G1 arrest into nocodazole. Using acrylamide gels containing Phos-tag reagent (Kinoshita et al., 2008), we observed that Cdc16 is already more highly phosphorylated in *cdc55Δ* cells compared with *CDC55* wild-type strains during G1 arrest (indicated by the arrows in Fig. 6 A, left). This difference became more evident in cells arrested for 2 and 3 h in nocodazole: in *cdc55Δ* cells we observed phosphorylation-dependent shifts that were completely missing in *CDC55* cells (Fig. 6 A, left), and that were sensitive to phosphatase treatment (not depicted). A shift that was sensitive to phosphatase treatment was also detected in standard Western blots of lysates from *cdc55Δ* cells (Fig. S5 D), confirming that Cdc16 underwent enhanced phosphorylation in the absence of $PP2A^{Cdc55}$. The same analysis with Cdc27 did not reveal major differences in the total level of phosphorylation between *CDC55* wild type and *cdc55Δ* cells (Fig. 6 A, right).

These data indicate that the protein phosphatase $PP2A^{Cdc55}$ directly or indirectly dephosphorylates Cdc16 and that these events could be critical to maintenance of checkpoint arrest and inhibition of adaptation.

Together, our results support a scenario where Cdc28/Clb phosphorylates and $PP2A^{Cdc55}$ dephosphorylates Cdc16. The final output of these opposing activities could be net phosphorylation, leading to adaptation, or net dephosphorylation, leading to mitotic arrest. If this hypothesis were correct, we would expect the loss of checkpoint arrest in *cdc55Δ* cells to be reversed in the presence of nonphosphorylatable Cdc16.

Although Cdc27 is not dephosphorylated by $PP2A^{Cdc55}$, the simultaneous presence of nonphosphorylatable Cdc27 and Cdc16 strongly decreases the ability of the single mutants to adapt (Rudner and Murray, 2000). For this reason, we tested the hypothesis by assessing spindle checkpoint activity in the triple mutant *cdc16-7A cdc27-5A cdc55Δ*. By following the kinetics of mitotic spindles and the stability of Pds1, we observed that, in contrast to *GAL1-MAD2 (3X) cdc55Δ* cells, *GAL1-MAD2 (3X) cdc16-6A cdc27-5A cdc55Δ* were arrested by the checkpoint and in fact were severely impaired in adaptation to the spindle checkpoint induced by Mad2 overexpression (Fig. 6, B–E). The fact that a minority of triple mutant cells eventually adapted, whereas no *cdc16-6A cdc27-5A* cells did, could be due to the presence of additional phosphorylation sites on the APC/C recognized by $PP2A^{Cdc55}$. Alternatively, $PP2A^{Cdc55}$ might also inhibit APC/C activation via other pathways, which are nevertheless less relevant than APC/C dephosphorylation. When Mad2 was not overexpressed, all three strains progressed through the cell cycle with similar kinetics (Fig. S5 E).

We conclude that increased phosphorylation of Cdc16 causes the checkpoint deficiency of *cdc55Δ* cells.

$PP2A^{Cdc55}$ inhibits adaptation independently of Cdc14

Our data indicate that during adaptation, $PP2A^{Cdc55}$ inhibits the transition into anaphase by dephosphorylating Cdc16. Previous data showed that during a regular cycle $PP2A^{Cdc55}$ delays anaphase by preventing Cdc14 release from the nucleolus (Queralt et al., 2006; Wang and Ng, 2006; Yellman and Burke, 2006). It is thus possible that during mitotic arrest $PP2A^{Cdc55}$ not only prevents adaptation by dephosphorylating APC/C, but also by inhibiting the release of Cdc14, which could help cells to transit into anaphase by silencing the checkpoint (Mirchenko and Uhlmann, 2010).

To test this possibility, we determined whether constitutive Cdc14 activity is sufficient to inactivate a nocodazole-induced checkpoint. We used the *net1Δ* mutant, where Cdc14 is constitutively released throughout the cell cycle. Our results show that *net1Δ* cells are checkpoint proficient, as indicated by the stability of Pds1 (Fig. 7 A). Notably, *cdc55Δ* cells, which also release Cdc14 prematurely, are instead checkpoint deficient (Fig. 7 B). The metaphase-to-anaphase transition is similar in the two mutants during an unperturbed cell cycle (Fig. S5, F and G). These results indicate that Cdc14 release alone is not sufficient to inactivate the checkpoint, and imply that $PP2A^{Cdc55}$ activity does not arrest cells in metaphase by preventing Cdc14 release.

We then tested whether Cdc14 activity is essential for adapting cells to enter anaphase. If this were the case, we would expect that inactivation of Cdc14 after checkpoint arrest would cause a permanent metaphase block. Because *CDC14* is an essential gene, we used the temperature-sensitive mutant *cdc14-1*, which produces a phosphatase that is inactivated after ∼30 min at 37°C (Akiyoshi and Biggins, 2010). In the absence of active Cdc14, cells arrest in anaphase with elongated spindles (Rock and Amon, 2009). To observe the effect of an incomplete activation of Cdc14, we also used a strain carrying a temperature-sensitive mutation of Cdc15, which causes partial release of Cdc14, but nevertheless arrests in anaphase (Rock and Amon, 2009). We activated the checkpoint in these temperature-sensitive mutants by overexpressing Mad2 from the *GAL1* promoter.

Cells were synchronized in G1 at 23°C and released in galactose to activate the checkpoint. To inactivate cdc14-1 and cdc15-2, the temperature was increased to 37°C, 2 h after the release when most of the cells had large buds. The strains carrying *cdc14-1* and *cdc15-2* degraded Pds1 and Clb2 and disassembled metaphase spindles with only a small delay compared with *GAL-MAD2 (3X)*, and in contrast to the adaptation-deficient *GAL-MAD2 (3X) cdc27-5A cdc16-6A* cells; Cdc14 and Cdc15 were clearly inactivated as cells accumulated in anaphase (Fig. 7, C and D). *GAL1-MAD2 cdc15-2* cells were slightly delayed compared with *GAL1-MAD2 cdc14-1* cells. As expected,

reagent. The same samples were loaded on standard 10% acrylamide gels to assess the total levels of Pgk1, Cdc16, and Cdc27. In the bottom panels, the fraction of phospho-specific shifts on P-tag gels was normalized to the total amount of protein. Error bars refer to standard errors of three independent experiments. (B–E) *GAL1-MAD2 (3X) PDS1-MYC18 cdc55Δ* (yAC1823), *GAL1-MAD2 (3X) PDS1-MYC18 cdc27-5A cdc16-6A* (yAC1675), and *GAL1-MAD2 (3X) PDS1-MYC18 cdc27-5A cdc16-6A cdc55Δ* (yAC1952) cells were arrested in G1 with α-factor and released in galactose. Samples were collected for IF (B) and Western blotting analysis (C–E). The data shown in B are from a single representative experiment out of three repeats. For the experiment shown, $n = 100$.

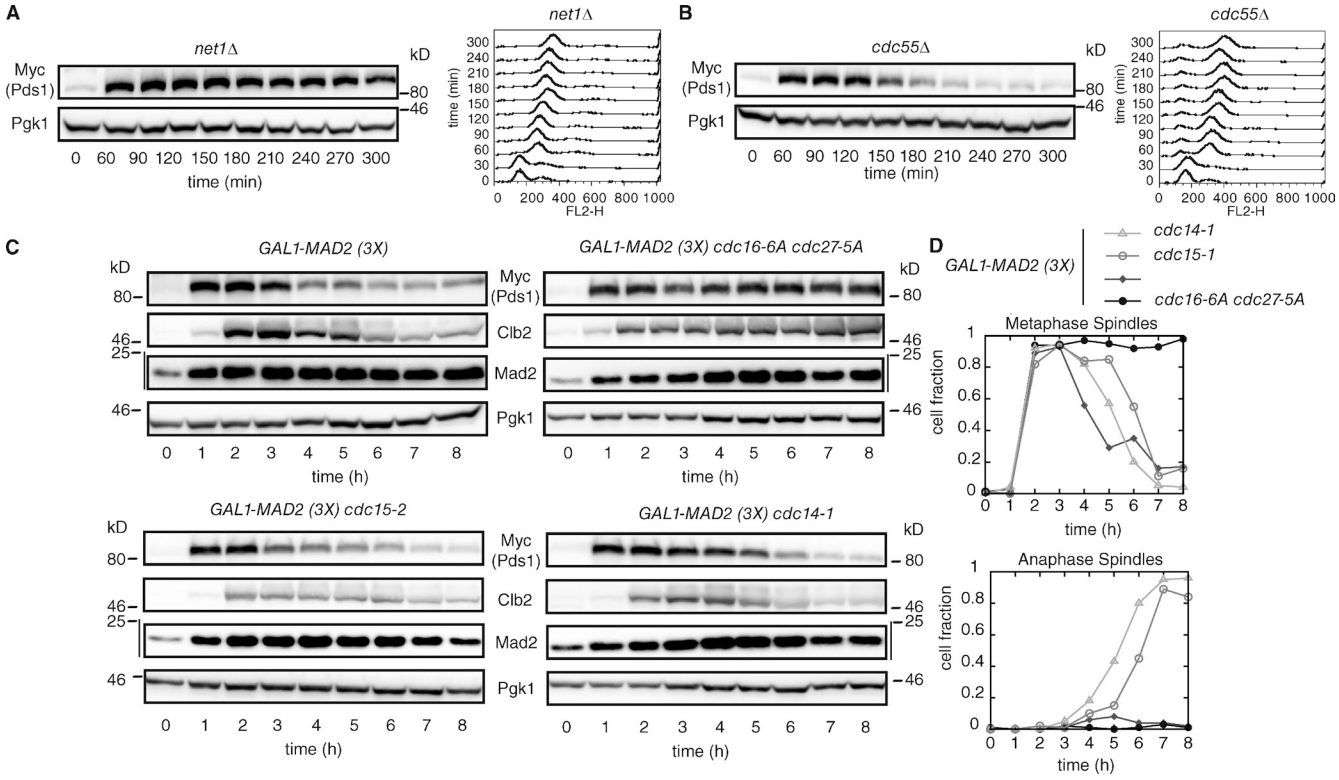

Figure 7. **Cdc14 is neither sufficient nor necessary to bypass the spindle checkpoint.** (A and B) *net1Δ PDS1-MYC18* (yAC1999) and *cdc55Δ PDS1-MYC18* (yAC1896) cells were grown at 25°C in YEPD, synchronized in G1 with α-factor, and released in the presence of nocodazole. 80 min after the release, when 90% of the cells were budded, α-factor was added again. Samples were collected for Western blotting and FACS. The data shown are from a single representative experiment out of three repeats. (C and D) *GAL1-MAD2 (3X) PDS1-MYC18* (yAC489), *GAL1-MAD2 (3X) PDS1-MYC18 cdc27-5A cdc16-6A* (yAC1675), *GAL1-MAD2 (3X) PDS1-MYC18 cdc14-1* (yAC1768), and *GAL1-MAD2 (3X) PDS1-MYC18 cdc15-2* (yAC1780) cells were grown in YEPR at 23°C. They were synchronized in G1 with α-factor and released into galactose. After 2 h, the cultures were shifted to 37°C and resupplemented with α-factor. Samples were collected for Western blotting (C) and IF (D). The data shown in D are from single representative experiments out of three repeats. For the experiments shown, $n = 100$.

when the same strains were released at 37°C in glucose (i.e., without switching on the *GAL1* promoter and inducing Mad2 overexpression), cells carrying the mutations in *CDC14* and *CDC15* showed metaphase spindle kinetics similar to wild-type cells before arresting in anaphase, whereas the double APC/C *cdc27-5A cdc16-6A* mutant was delayed by ∼20 min in the exit from metaphase (Fig. S5 H).

We conclude that Cdc14 activation is not necessary for cells to transit into anaphase when the checkpoint is activated.

Discussion

When cells are exposed to prolonged checkpoint-inducing stimuli, they are arrested in metaphase by the sequestration of the APC/C cofactor, Cdc20, in the MCC. After several hours, cells eventually adapt to the stimulus, resulting in segregation of their DNA material and exit from mitosis. Because Cdc20 is sequestered in the MCC during a checkpoint arrest, it is unclear how APC/C is activated during adaptation to drive cells into anaphase.

Molecular mechanisms for adaptation to the spindle checkpoint

One possibility is that APC/C bypasses the requirement for Cdc20 during adaptation. Our data show that Cdh1, the other APC/C cofactor, is dispensable for adaptation to the spindle checkpoint, as also suggested by Rossio et al. (2010) and Rudner et al. (2000). A second option is that cells adapt because they switch off the checkpoint cascade. However, we did not obtain any evidence to support such a scenario. Previous studies in budding yeast suggest that the pathway upstream of MCC formation is switched off via a decrease of Mad1/Bub3 binding (Rossio et al., 2010), two components of the spindle checkpoint pathway that localize at the kinetochores. In our adaptation experiments, we have activated the checkpoint ectopically by overexpressing Mad2. We have shown previously that in this setting MCC formation occurs independently from Mad1 (Mariani et al., 2012) and thus the reduced binding of Mad1 with Bub3 is unlikely to lead to the release of Cdc20 from the MCC. It was also reported that Bub1 degradation helps adaptation (Goto et al., 2011), but we have previously shown that Bub1 does not localize to kinetochores in cells overexpressing Mad2 (Mariani et al., 2012). For this reason, we suspect that Bub1 inactivation does not underlie adaptation in our system. Another attractive candidate for checkpoint silencing is Cdc14, given its recently discovered role in preventing checkpoint reactivation in anaphase (Mirchenko and Uhlmann, 2010). However, we determined that Cdc14 was neither necessary nor sufficient for adapting cells to transit into anaphase. Cdc28 inactivation might

also underlie checkpoint inactivation at the time of adaptation, as has been proposed to occur during the transition to anaphase in vertebrates (Zeng et al., 2010; He et al., 2011). However, we observed that the inhibition of Cdc28 does not delocalize Mad2 from the kinetochores in yeast cells arrested in prometaphase by the checkpoint, which suggests that in yeast there is not such a strong link between Cdc28 activity and checkpoint maintenance. Moreover, we demonstrated that inhibition of Cdc28 activity in checkpoint-arrested cells is incompatible with transition into anaphase. In conclusion, our data support the notion that adaptation takes place when the checkpoint is fully functional as originally proposed by Brito and Rieder (2006).

In this scenario, adaptation would be driven by a mechanism that competes with the checkpoint and eventually overrides it through the formation of a critical amount of APC/C^{Cdc20} that drives cells into anaphase. Here, we propose that the phosphorylation of APC/C, favored by Cdc28 and opposed by $PP2A^{Cdc55}$, plays a critical role in the adaptation process. The observation that the mitotic cyclin Clb2, a key regulator of Cdc28, accumulates steadily before cells adapt, supports the idea that a threshold level of active APC/C phosphorylation needs to be reached before cells can overcome checkpoint arrest. Possibly, APC/C phosphorylation drives the formation of APC/C^{Cdc20} because it increases the affinity of APC/C for Cdc20 (Rudner and Murray, 2000). Although we demonstrate that APC/C phosphorylation is necessary for adaptation, we cannot conclude that it is the ultimate event that causes it. Further work is needed to clarify this point, and particularly to study the regulation of $PP2A^{Cdc55}$ in adapting cells. Whatever the mechanism that triggers adaptation, the high variability in adaptation times complicates the analysis of this process.

It is worthwhile to note that in mammals the molecular mechanism that drives adaptation is likely to differ from that in yeast. Indeed, it has been shown that during adaptation in single mammalian cells cyclin B is slowly degraded (Brito and Rieder, 2006), which is at variance with our results in single budding yeast cells.

The interplay of $PP2A^{Cdc55}$ and Cdc28/Clb2 controls checkpoint proficiency

Our data provide a new explanation for the old observation that the regulatory subunit of the PP2A phosphatase, Cdc55, is required for the spindle checkpoint. We suggest that $PP2A^{Cdc55}$ contributes to checkpoint arrest by inhibiting the formation of APC/C^{Cdc20} through the dephosphorylation of the APC/C subunit, Cdc16. In this scenario, cells lacking Cdc55 would "always be adapted" because the inability to dephosphorylate APC/C would render cells unable to mount a checkpoint arrest. Accordingly, *cdc55Δ* cells become checkpoint proficient again in a strain where the phosphorylation sites of Cdc16 and Cdc27 recognized by Cdc28/Clb2 are mutated to alanine. This result sheds light on a previous observation that a *CDC28* mutant with decreased kinase activity (*CDC28-VF*) rescues the checkpoint defect of *cdc55Δ* (Minshull et al., 1996). In our interpretation, the rescue is caused by a balancing out of APC/C phosphorylation and dephosphorylation, achieved by the simultaneous decrease of Cdc28 kinase and PP2A phosphatase activity.

Our results showing that $PP2A^{Cdc55}$ dephosphorylates Cdc16, which are in agreement with recent findings (Lianga et al., 2013), do not exclude the existence of phosphatases other than $PP2A^{Cdc55}$ that could dephosphorylate APC/C. The phosphorylation state of Cdc27 is not affected by the deletion of *CDC55*, and yet the alanine substitution of the phosphorylation sites on Cdc27 decreases the capability of cells to adapt (Rudner and Murray, 2000). Moreover, the previous observation that the deletion of *CDC55* is fully balanced by the partial inhibition of Cdc28 (Minshull et al., 1996) could be explained by the presence of overlapping phosphatases.

A positive feedback loop controlling APC/C^{Cdc20} activation during adaptation

During adaptation, activation of APC/C^{Cdc20} requires Cdc28/Clbs. Consistently, Clb2 accumulates in the nucleus steadily for several hours until cells adapt. However, as soon as APC/C^{Cdc20} is activated it rapidly degrades Clb2: the high level of Cdc28/Clbs that cells accumulated in several hours is lost in a few minutes (Fig. 5 A). The later stages of Clb2 degradation are likely due to APC/C^{Cdh1}, but the initial stages are APC/C^{Cdc20} dependent, and are aided by APC/C phosphorylation. It is therefore surprising that the rapidly diminishing levels of Cdc28/Clbs are able to sustain efficient phosphorylation of APC/C, in the initial stages after APC/C^{Cdc20} activation, in the presence of the counteracting phosphatase $PP2A^{Cdc55}$.

This conundrum does not concern only adaptation in budding yeast. In cycling extracts of *Xenopus laevis*, it was recently shown that this paradox is resolved by a time delay between CDK1 and APC/C^{Cdc20} activation, which guarantees high levels of APC/C^{Cdc20} after it starts to degrade Cyclin B (Yang et al., 2013). Our data suggest a possible molecular mechanism to explain the establishment of the time delay. During a regular transition to anaphase, $PP2A^{Cdc55}$ is inhibited by separase (Queralt et al., 2006), which is in turn activated by APC/C^{Cdc20}. Together, these proteins form a positive feedback loop (APC/C^{Cdc20} ⊣ Securin ⊣ separase ⊣ $PP2A^{Cdc55}$ ⊣ APC/C^{Cdc20}) that is coupled to the negative feedback loop, whereby APC/C^{Cdc20} inactivates Cdc28/Clbs that in turn activates APC/C (Fig. 8 A). A simple model based on these ideas (see Materials and methods) shows that Clb2 increases steadily until APC/C is activated, and then the negative feedback loop comes into action (Fig. 8 B). After this point, APC/C^{Cdc20} locks APC/C in the phosphorylated state by inhibiting the protein phosphatase responsible for APC/C dephosphorylation. Hereafter, the decrease of Cdc28/Clb2 activity becomes irrelevant, as the phosphatase that could oppose Cdc28 activity has been inactivated. In fact, APC/C^{Cdc20} activity stays high after Clb2 is long gone (in reality it will likely be removed, together with the remaining Clb2, by APC/C^{Cdh1}, which is missing in the model).

Our model is based on the idea that the positive feedback loop creates two states (i.e., it is bistable): a metaphase state with APC/C^{Cdc20} inactive and $PP2A^{Cdc55}$ active, and an anaphase state that follows adaptation where the activation states are reversed. The idea that a bistable switch controls transition into anaphase is not new. It was proposed for the first time after the observation that APC/C^{Cdc20} degrades Mps1, a component of

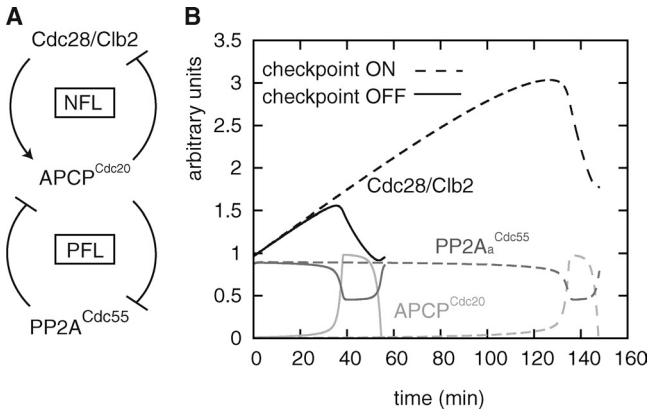

Figure 8. **A simple model for the metaphase-to-anaphase transition in adaptation.** (A) APC/C^{Cdc20}, Cdc28/Clbs, and $PP2A^{Cdc55}$ give rise to a positive feedback loop (PFL) and a negative feedback loop (NFL). (B) The dynamics of the model are shown starting from the lowest Clb2 levels in both a regular transition to anaphase (solid line) and during adaptation (broken line; decreased activation rate of APC). See also Materials and methods.

the checkpoint (Palframan et al., 2006). In that case, inactive APC/C^{Cdc20} and active Mps1 characterized metaphase, whereas the activation states were swapped in anaphase. Other positive feedback loops have been proposed more recently to govern the transition (Zeng et al., 2010; He et al., 2011). Currently, it is not known how these switches cooperate with each other, and in fact more data are needed to confirm the relevance of a bistable switch controlling the transition to anaphase in budding yeast.

Materials and methods

Strains, media, and reagents

Strains used in this study are listed in Table S1. All yeast strains were derivatives of or were backcrossed at least three times with W303 (*ade2-1*, *trp1-1*, *leu2-3*, *112*, *his3-11*, *15*, *ura3*, and *ssd1*). *cdc27-5A* and *cdc16-6A* mutants were obtained from A. Murray (Department of Molecular and Cellular Biology and Center for Systems Biology, Harvard University, Cambridge, MA); *cdc28-as1* and *yox1Δ* were received from U. Surana (Institute of Molecular and Cell Biology, Agency for Science, Technology and Research [A*STAR], Singapore); *cdc14-1*, *cdc15-2*, and *GAL1-SIC1* were from R. Visintin (IEO, Milan, Italy); and the original construct for *GAL1-MAD2* was developed in the lab of S. Piatti (Centre de Recherche en Biochimie Macromoléculaire, Montpellier, France).

The population experiment in Fig. S1 B was performed in synthetic medium lacking methionine. All other population experiments were performed using YEP medium (1% yeast extract, 2% Bacto Peptone, and 50 mg/liter adenine) supplemented with 2% glucose (YEPD), 2% raffinose (YEPR), or 2% raffinose and 2% galactose (YEPRG). Single cell adaptation experiments under Mad2 overexpression were performed using synthetic complete medium supplemented with ammonium sulfate.

α-Factor and nocodazole were used at 5 µg/ml and 15 µg/ml, respectively. α-Factor readdition was at 20 µg/ml. Methionine was added at a final concentration of 20 mM to repress the *MET3* promoter. Unless otherwise specified, all experiments were performed at 30°C. In population experiments of adaptation, galactose was added 1 h before the release from α-factor (20 min for Fig. S1 B), while α-factor was re-added 1.5–2 h after the release from G1, unless otherwise stated.

Western blot analysis

In all Western blot experiments, samples were collected at the indicated time points, and cells were pelleted by centrifugation for 2 min at room temperatures. Then 100 µl TCA was added to the pellets to precipitate proteins. TCA protein extracts were prepared according to Fraschini et al. (1999). Protein samples were loaded and separated in 10% or 12.5% polyacrylamide gels (with a bis-acrylamide/acrylamide ratio of 1:29) with the voltage of separation apparatuses set to 140 V. For detection of Cdc16 and Cdc27 phosphorylation-specific bands, the Phos-tag system (50 µM Phos-tag reagent) was used (Kinoshita et al., 2008). To visualize phosphorylation shifts of Cdc16 on normal gels, we prepared 7.5% polyacrylamide gels with a bis-acrylamide/acrylamide ratio of 1:80. Proteins were transferred from gels to Protran membranes for 1 h, with transfer apparatuses set at 100 V. For the detection of Myc-tagged proteins (Pds1-Myc18, Cdc16-Myc6, and Cdc27-Myc9; the last two strains were a gift from J.-M. Peters, Research Institute of Molecular Pathology [IMP], Vienna, Austria) and of Mad2, membranes were probed, respectively, with 9E10 anti-Myc and anti-ScMad2 antibodies produced at the Monoclonal Antibodies Facility at the IFOM-IEO Campus (1:1,000 dilution). Commercial antibodies were used as follows: Cdc20 (yC-20; Santa Cruz Biotechnology, Inc.) at 1:1,000, Clb2 (y180; Santa Cruz Biotechnology, Inc.) at 1:1,000, and Pgk1 (D660; Invitrogen) at 1:5,000. Secondary antibodies were from Bio-Rad Laboratories and proteins were detected by an enhanced chemiluminescence system (Pierce ECL; Thermo Fischer Scientific) according to the manufacturer's instructions. Blots were acquired as digitalized images by a Chemidoc XRS+System (Bio-Rad Laboratories) and the software Imagelab was used to quantify the signals. Molecular weights in the Western blot panels refer to Prestained Protein Marker (New England Biolabs, Inc.) bands run on the same blot.

To quantify Cdc16 and Cdc27 phospho-specific bands on P-Tag gels, the signal corresponding to the phosphorylation shift (above the second band visible during the G1-arrest) was normalized over the total amount of protein in the same gel at the same time point.

Other techniques

Flow cytometric DNA quantitation was determined using a flow cytometer (FACScan or FACScalibur; BD) and analyzed with FlowJO Software. For each sample, we scored 10,000 events.

Metaphase and anaphase spindles (i.e., immunofluorescence [IF] analysis) were detected by α-tubulin immunostaining with the YOL34 monoclonal antibody (AbD Serotec) followed by indirect IF using FITC-conjugated anti–rat antibody (Jackson ImmunoResearch Laboratories, Inc.).

Single cell analysis was performed using microfluidic chambers (CELLASIC), with cells growing at 30°C in synthetic medium containing raffinose. Time-lapse movies were recorded using a DeltaVision Elite imaging system (Applied Precision) based on an inverted microscope (IX71; Olympus) with a camera (CoolSNAP HQ2; Photometrics) and a UPlan-Apochromat 60× (1.4 NA) oil immersion objective lens (Olympus). Cells expressing Mad2-3GFP (gift from T. Tanaka, Centre for Gene Regulation and Expression, College of Life Sciences, University of Dundee, Scotland, UK) and Nuf2-mCherry (a gift from S. Westermann, Research Institute of Molecular Pathology [IMP], Vienna, Austria) were fixed in cold 100% ethanol, and images were acquired on the DeltaVision Elite imaging system using a UPlan-Apochromat 100× (1.4 NA) oil immersion objective lens (Olympus). We counted cells as colocalized where the maximum of Mad2-GFP signal was localized with one Nuf2-mCherry dot.

To perform the phosphatase assay on protein samples extracted with TCA, Laemmli buffer was exchanged with Buffer3 (10 mM $MgCl_2$, 100 mM NaCl, 50 mM TRIS, and 1 mM DTT, pH 7.9) using Amicon Ultra centrifugal filters (Millipore). The extracts were then incubated for 30 min at 37°C with buffer alone, calf intestinal phosphates (CIP; New England Biolabs, Inc.), or CIP plus 10 mM sodium orthovanadate (to inhibit the CIP).

Methods for image analysis

Segmentation and whole-cell signal. Image analysis was performed with software written in MATLAB (MathWorks). For the segmentation and tracking of yeast cells we used the program phyloCell, written by G. Charvin (Institut de Génétique et de Biologie Moléculaire et Cellulaire, Illkirch, France). From the fluorescent signal of the whole cell we subtracted a background signal that we obtained from cells not carrying the fluorescent markers grown in the same conditions. We observed a slight increase in autofluorescence during adaptation and corrected our measurements accordingly.

Nuclear signal. The calculation of the concentration of fluorescence in the nucleus required us to know the area of the nucleus. Because our cells do not carry a nuclear marker, we used the Clb2-GFP signal itself, as Clb2 accumulates in the nucleus during mitosis. The identification of the nucleus was thus successful only when the intensity of the Clb2 nuclear signal was significantly higher than in the rest of the cell. The size of the nucleus could then be identified by k-means clustering, using k = 3 (the clusters corresponding to nucleus, cytoplasm, and extracellular region; see Video 1). In contrast, when the intensities in the nucleus and in the cytoplasm were

similar, the clustering gave unrealistically high values for the size of the nucleus. Therefore, the moment in which the measurement becomes reliable is marked by a drop in the ratio of the size of the nuclear cluster to the size of the whole cell (Fig. S4 B, top). We considered the clustering to be reliable when this ratio was below a value of 30%. We used the nuclear signal for our calculations only in this region (Fig. S4 B, bottom, solid line), after smoothing using a moving average. For the sake of representation, in Fig. 5 A and Fig. S4 C we also plotted the nuclear concentrations when the definition of the nucleus was unreliable.

The signal before interpolation is visible in Video 1.

Expression rate. We observed that the increase in nuclear Clb2, both in cycling cells and in the initial phase of adaptation, was approximately linear. Therefore, to quantify the expression rates (Fig. 5 B, top right), we performed a linear fit and compared the resulting slopes for the two conditions. We only used the part of the curve where the increase was sufficiently linear and for which the measurement of the nuclear region was reliable (see "Nuclear signal").

Degradation rate. It was not possible to measure the rate of Clb2 degradation in adapting cells directly in the nucleus because the measurement of the nuclear region was not reliable during the degradation phase. For this reason we analyzed Clb2 degradation using the mean fluorescence in the whole cell (Fig. 5 B, top left). We assumed that this degradation can be described by a simple exponential decay (Fig. S4 A, top) and that at the end of the process Clb2 is fully degraded.

Maxima. The maxima of fluorescence (Fig. 5 B, bottom left) were measured by taking the local maxima of nuclear fluorescence in the case of cycling cells. In the case of the adapting cells, we took the highest fluorescence level after smoothing that was reached during the adaptation process.

Adaptation time. Adaptation time (Fig. 5 B, bottom right) was measured in cells adapting to Mad2 overexpression as the time that elapses between the moment Clb2 starts to accumulate to the time the mitotic spindle elongates. If the time of spindle elongation was uncertain, we chose the beginning of Clb2 degradation. When we analyzed adaptation of cells treated with nocodazole (Fig. S4 C, top), we obviously chose only cells that had not formed clusters of tubulin by the time of Clb2 degradation, and thus we did not take into account cells that degraded Clb2 after tubulin reappeared (Fig. S4 C, bottom).

Mathematical model

Because Cdc28 is present in excess over Clb2 and their binding is spontaneous, in the model we follow the dynamics of Clb2 as a readout for the complex Cdc28/Clb2. As for APC/C, we did not explicitly introduce Cdc20 but we assume that Cdc20 binds efficiently to phosphorylated APC/C (i.e., APCP comes always with Cdc20 bound to it and is a readout for APC/C^{Cdc20}). As for $PP2A^{Cdc55}$, given that the mechanism whereby separase degradation induces the inhibition of the phosphatase is not known, we simply introduce two species, active and inactive. Simulations were performed with XPPAUT. To produce the behavior shown in Fig. 8, we required the model to be in a limit cycle solution. The parameter values have been chosen accordingly (i.e., any other choice of parameter that produces a limit cycle solution would equally prove the point). Similarly, initial conditions were chosen from the limit cycle solution with kph = 1.2 (i.e., checkpoint OFF) where Clb2 concentration was minimal. In the checkpoint ON condition, kph = 0.6, which implies reduced APC/C^{Cdc20} formation. In the following sections, we describe the reactions of the model, and the corresponding mathematical formalism (i.e., algebraic and differential equations).

Reactions. The model includes the following reactions.

APC + Clb2 → APCP + Clb2 (kph = phosphorylation; Japc = Michaelis constant for APCP phosphorylation)

APCP + Cdc55a → APC + Cdc55a (kdeph = dephosphorylation; Japci = Michaelis constant for APCP dephosphorylation)

Cdc55i → Cdc55a (ka = Cdc55 activation)

Cdc55a + APCP → Cdc55i + APCP (ki = Cdc55 inactivation)

→ Cdc20 (ksyn = Cdc20 synthesis)

Cdc20 + APCP → APCP (kdeg = Cdc20 degradation)

When translated in mathematical formalism, the reactions produce the following algebraic-differential equations.

Algebraic equations. The following equations were used.

APC = APCtot − APCP

Cdc55i = Cdc55tot − Cdc55a

Differential equations. Molecular species that could not be identified with algebraic equations were numerically computed using the following differential equations.

dAPCP/dt = (APC × kph × Clb2)/(Japc+APC) − [APCP × (kdeph × Cdc55a)]/(Japci + APCP)

dCdc55a/dt = ka × Cdc55i-Cdc55a × (ki × APCP)

dClb2/dt = ksyn − Clb2 × (kdeg × APCP)

Parameters.

1/min parameters.

APC/C phosphorylation: kph = 0.6 (checkpoint ON), kph = 1.2 (checkpoint OFF)

APC/C dephosphorylation: kdeph = 2.4

$PP2A^{Cdc55}$ activation: ka = 1.2

$PP2A^{Cdc55}$ inactivation: ki = 1.2

Cdc20 synthesis: ksyn = 0.02

Cdc20 degradation: kdeg = 0.055

Dimensionless parameters.

Michaelis constant for APC/C activation: Japc = 0.01

Michaelis constant for APC/C inactivation: Japci = 0.01

Total APC/C: APCtot = 1

Total Cdc55: Cdc55tot = 0.9

Initial conditions (dimensionless). Initial conditions were as follows.

APCP = 0.012, Cdc55A = 0.875, Clb2 = 0.965

Online supplemental material

Fig. S1 shows that Cdc28 inhibition arrests cells in mitosis with an active checkpoint. Fig. S2 shows that partial inhibition of Cdc28 does not destabilize Pds1 and Clb2 in the presence of Cdc20. Fig. S3 shows that 50 nM of 1-NMPP1 only mildly delays cell cycle progression. Fig. S4 shows single cell analysis of Clb2 accumulation during a checkpoint-arrest. Fig. S5 shows that Cdc16 phosphorylation induces a gel shift during a prolonged spindle checkpoint arrest, and that Cdc14 is not required for adaptation. Table S1 is a strain list. Video 1 shows the signal of Clb2-GFP and TUB2-Cherry in one adapting cell and the definition of the nuclear volume after clustering. Online supplemental material is available at http://www.jcb.org/cgi/content/full/jcb.201303033/DC1.

We thank Luca Mariani and Emanuele Martini for helping at different stages of this project; Andrew Murray, Jan Michael Peters, Simonetta Piatti, Pamela Silver, Uttam Surana, Tomo Tanaka, Rosella Visintin, and Stefan Westermann for reagents and strains; Rosalind Gunby, Andrea Musacchio, Simonetta Piatti, and Rosella Visintin for discussions and comments on the manuscript; Fred Cross for introducing us to single cell analysis; and the imaging facility of the IFOM-IEO campus.

The group of Andrea Ciliberto is financed by the Associazione Italiana Ricerca sul Cancro (AIRC) and Regione Lombardia (DIVA). Elena Chiroli benefits of a fellowship from Fondazione Veronesi.

Submitted: 7 March 2013
Accepted: 31 July 2013

References

Akiyoshi, B., and S. Biggins. 2010. Cdc14-dependent dephosphorylation of a kinetochore protein prior to anaphase in *Saccharomyces cerevisiae*. *Genetics*. 186:1487–1491. http://dx.doi.org/10.1534/genetics.110.123653

Amon, A. 1997. Regulation of B-type cyclin proteolysis by Cdc28-associated kinases in budding yeast. *EMBO J.* 16:2693–2702. http://dx.doi.org/10.1093/emboj/16.10.2693

Bishop, A.C., J.A. Ubersax, D.T. Petsch, D.P. Matheos, N.S. Gray, J. Blethrow, E. Shimizu, J.Z. Tsien, P.G. Schultz, M.D. Rose, et al. 2000. A chemical switch for inhibitor-sensitive alleles of any protein kinase. *Nature*. 407:395–401. http://dx.doi.org/10.1038/35030148

Brito, D.A., and C.L. Rieder. 2006. Mitotic checkpoint slippage in humans occurs via cyclin B destruction in the presence of an active checkpoint. *Curr. Biol.* 16:1194–1200. http://dx.doi.org/10.1016/j.cub.2006.04.043

Clift, D., F. Bizzari, and A.L. Marston. 2009. Shugoshin prevents cohesin cleavage by PP2A(Cdc55)-dependent inhibition of separase. *Genes Dev.* 23:766–780. http://dx.doi.org/10.1101/gad.507509

D'Angiolella, V., C. Mari, D. Nocera, L. Rametti, and D. Grieco. 2003. The spindle checkpoint requires cyclin-dependent kinase activity. *Genes Dev.* 17:2520–2525. http://dx.doi.org/10.1101/gad.267603

Drapkin, B.J., Y. Lu, A.L. Procko, B.L. Timney, and F.R. Cross. 2009. Analysis of the mitotic exit control system using locked levels of stable mitotic cyclin. *Mol. Syst. Biol.* 5:328. http://dx.doi.org/10.1038/msb.2009.78

Fraschini, R., E. Formenti, G. Lucchini, and S. Piatti. 1999. Budding yeast Bub2 is localized at spindle pole bodies and activates the mitotic checkpoint via

a different pathway from Mad2. *J. Cell Biol.* 145:979–991. http://dx.doi.org/10.1083/jcb.145.5.979

Gillett, E.S., C.W. Espelin, and P.K. Sorger. 2004. Spindle checkpoint proteins and chromosome-microtubule attachment in budding yeast. *J. Cell Biol.* 164:535–546. http://dx.doi.org/10.1083/jcb.200308100

Goto, G.H., A. Mishra, R. Abdulle, C.A. Slaughter, and K. Kitagawa. 2011. Bub1-mediated adaptation of the spindle checkpoint. *PLoS Genet.* 7: e1001282. http://dx.doi.org/10.1371/journal.pgen.1001282

He, E., O. Kapuy, R.A. Oliveira, F. Uhlmann, J.J. Tyson, and B. Novák. 2011. System-level feedbacks make the anaphase switch irreversible. *Proc. Natl. Acad. Sci. USA*. 108:10016–10021. http://dx.doi.org/10.1073/pnas.1102106108

Hood, J.K., W.W. Hwang, and P.A. Silver. 2001. The *Saccharomyces cerevisiae* cyclin Clb2p is targeted to multiple subcellular locations by cis- and trans-acting determinants. *J. Cell Sci.* 114:589–597.

Kinoshita, E., E. Kinoshita-Kikuta, M. Matsubara, S. Yamada, H. Nakamura, Y. Shiro, Y. Aoki, K. Okita, and T. Koike. 2008. Separation of phosphoprotein isotypes having the same number of phosphate groups using phosphate-affinity SDS-PAGE. *Proteomics*. 8:2994–3003. http://dx.doi.org/10.1002/pmic.200800243

Kitazono, A.A., D.A. Garza, and S.J. Kron. 2003. Mutations in the yeast cyclin-dependent kinase Cdc28 reveal a role in the spindle assembly checkpoint. *Mol. Genet. Genomics*. 269:672–684. http://dx.doi.org/10.1007/s00438-003-0870-y

Lara-Gonzalez, P., F.G. Westhorpe, and S.S. Taylor. 2012. The spindle assembly checkpoint. *Curr. Biol.* 22:R966–R980. http://dx.doi.org/10.1016/j.cub.2012.10.006

Li, X., and M. Cai. 1997. Inactivation of the cyclin-dependent kinase Cdc28 abrogates cell cycle arrest induced by DNA damage and disassembly of mitotic spindles in *Saccharomyces cerevisiae*. *Mol. Cell. Biol.* 17: 2723–2734.

Liang, H., H.H. Lim, A. Venkitaraman, and U. Surana. 2012. Cdk1 promotes kinetochore bi-orientation and regulates Cdc20 expression during recovery from spindle checkpoint arrest. *EMBO J.* 31:403–416. http://dx.doi.org/10.1038/emboj.2011.385

Lianga, N., E.C. Williams, E.K. Kennedy, C. Doré, S. Pilon, S.L. Girard, J.S. Deneault, and A.D. Rudner. 2013. A Wee1 checkpoint inhibits anaphase onset. *J. Cell Biol.* 201:843–862. http://dx.doi.org/10.1083/jcb.201212038

Mariani, L., E. Chiroli, L. Nezi, H. Muller, S. Piatti, A. Musacchio, and A. Ciliberto. 2012. Role of the Mad2 dimerization interface in the spindle assembly checkpoint independent of kinetochores. *Curr. Biol.* 22:1900–1908. http://dx.doi.org/10.1016/j.cub.2012.08.028

Minshull, J., A. Straight, A.D. Rudner, A.F. Dernburg, A. Belmont, and A.W. Murray. 1996. Protein phosphatase 2A regulates MPF activity and sister chromatid cohesion in budding yeast. *Curr. Biol.* 6:1609–1620. http://dx.doi.org/10.1016/S0960-9822(02)70784-7

Mirchenko, L., and F. Uhlmann. 2010. Sli15(INCENP) dephosphorylation prevents mitotic checkpoint reengagement due to loss of tension at anaphase onset. *Curr. Biol.* 20:1396–1401. http://dx.doi.org/10.1016/j.cub.2010.06.023

Morin, V., S. Prieto, S. Melines, S. Hem, M. Rossignol, T. Lorca, J. Espeut, N. Morin, and A. Abrieu. 2012. CDK-dependent potentiation of MPS1 kinase activity is essential to the mitotic checkpoint. *Curr. Biol.* 22:289–295. http://dx.doi.org/10.1016/j.cub.2011.12.048

Nasmyth, K. 2002. Segregating sister genomes: the molecular biology of chromosome separation. *Science*. 297:559–565. http://dx.doi.org/10.1126/science.1074757

Palframan, W.J., J.B. Meehl, S.L. Jaspersen, M. Winey, and A.W. Murray. 2006. Anaphase inactivation of the spindle checkpoint. *Science*. 313:680–684. http://dx.doi.org/10.1126/science.1127205

Pan, J., and R.H. Chen. 2004. Spindle checkpoint regulates Cdc20p stability in *Saccharomyces cerevisiae*. *Genes Dev.* 18:1439–1451. http://dx.doi.org/10.1101/gad.1184204

Primorac, I., and A. Musacchio. 2013. Panta rhei: the APC/C at steady state. *J. Cell Biol.* 201:177–189. http://dx.doi.org/10.1083/jcb.201301130

Queralt, E., C. Lehane, B. Novak, and F. Uhlmann. 2006. Downregulation of PP2A(Cdc55) phosphatase by separase initiates mitotic exit in budding yeast. *Cell*. 125:719–732. http://dx.doi.org/10.1016/j.cell.2006.03.038

Rieder, C.L., R.W. Cole, A. Khodjakov, and G. Sluder. 1995. The checkpoint delaying anaphase in response to chromosome monoorientation is mediated by an inhibitory signal produced by unattached kinetochores. *J. Cell Biol.* 130:941–948. http://dx.doi.org/10.1083/jcb.130.4.941

Rock, J.M., and A. Amon. 2009. The FEAR network. *Curr. Biol.* 19:R1063–R1068. http://dx.doi.org/10.1016/j.cub.2009.10.002

Rossio, V., E. Galati, M. Ferrari, A. Pellicioli, T. Sutani, K. Shirahige, G. Lucchini, and S. Piatti. 2010. The RSC chromatin-remodeling complex influences mitotic exit and adaptation to the spindle assembly checkpoint by controlling the Cdc14 phosphatase. *J. Cell Biol.* 191:981–997. http://dx.doi.org/10.1083/jcb.201007025

Rudner, A.D., and A.W. Murray. 2000. Phosphorylation by Cdc28 activates the Cdc20-dependent activity of the anaphase-promoting complex. *J. Cell Biol.* 149:1377–1390. http://dx.doi.org/10.1083/jcb.149.7.1377

Rudner, A.D., K.G. Hardwick, and A.W. Murray. 2000. Cdc28 activates exit from mitosis in budding yeast. *J. Cell Biol.* 149:1361–1376. http://dx.doi.org/10.1083/jcb.149.7.1361

Schwob, E., T. Böhm, M.D. Mendenhall, and K. Nasmyth. 1994. The B-type cyclin kinase inhibitor p40SIC1 controls the G1 to S transition in *S. cerevisiae*. *Cell*. 79:233–244. http://dx.doi.org/10.1016/0092-8674(94)90193-7

Wang, Y., and T.Y. Ng. 2006. Phosphatase 2A negatively regulates mitotic exit in *Saccharomyces cerevisiae*. *Mol. Biol. Cell*. 17:80–89. http://dx.doi.org/10.1091/mbc.E04-12-1109

Yang, Q., and J.E. Ferrell Jr. 2013. The Cdk1-APC/C cell cycle oscillator circuit functions as a time-delayed, ultrasensitive switch. *Nat. Cell Biol.* 15:519–525. http://dx.doi.org/10.1038/ncb2737

Yellman, C.M., and D.J. Burke. 2006. The role of Cdc55 in the spindle checkpoint is through regulation of mitotic exit in *Saccharomyces cerevisiae*. *Mol. Biol. Cell*. 17:658–666. http://dx.doi.org/10.1091/mbc.E05-04-0336

Zachariae, W., M. Schwab, K. Nasmyth, and W. Seufert. 1998. Control of cyclin ubiquitination by CDK-regulated binding of Hct1 to the anaphase promoting complex. *Science*. 282:1721–1724. http://dx.doi.org/10.1126/science.282.5394.1721

Zeng, X., F. Sigoillot, S. Gaur, S. Choi, K.L. Pfaff, D.C. Oh, N. Hathaway, N. Dimova, G.D. Cuny, and R.W. King. 2010. Pharmacologic inhibition of the anaphase-promoting complex induces a spindle checkpoint-dependent mitotic arrest in the absence of spindle damage. *Cancer Cell*. 18:382–395. http://dx.doi.org/10.1016/j.ccr.2010.08.010